A multitarget range-azimuth tracker for maritime applications

Francesco Bandiera, Marco Del Coco, and Giuseppe Ricci
University of Salento, Dipartimento di Ingegneria dell'Innovazione
Via Monteroni, 73100 Lecce (LE), Italy
E-Mail: name.surname@unisalento.it

***Abstract*—In this paper, we focus on the design of a Kalman filter-based algorithm to track multiple targets in range and azimuth. The detection stage implements a multitarget strategy and is aimed at collecting and eventually processing all target components (i.e., in range and azimuth). Existing tracks are updated using a JPDA to handle the data association problem. We model target echoes as coherent pulse trains in white Gaussian noise with unknown power. The performance analysis assumes a maritime scenario and shows that the proposed tracker outperforms more conventional approaches.**

I. Introduction

Tracking algorithms rely on a detection stage that provides a set of point measurements at each scan; most detectors considered so far assume that the target is located exactly "where the matched filter is sampled" and, hence, that there is no spillover of target energy to adjacent matched filter samples. However, the spillover is taken into account in [1] where the case of several closely spaced targets, ruled by a Swerling 2 model, that fall within the same beam of a monopulse radar and among three or more adjacent matched filter samples in range, is considered; therein, a maximum likelihood (ML) extractor is developed. The idea is further investigated in order to estimate the angles and ranges of multiple unresolved extended targets in [2]. In [3] an adaptive space-time detector is derived and assessed: it takes advantage of the possible spillover of target energy for the case of coherent target echoes. In [4] this idea has been extended to address localization of multiple point-like targets within the same range cell or range cells in spatial proximity; therein, it is shown that the multitarget approach outperforms the corresponding single target one in the localization of a weak target for the case of targets with different strength. In [5], a Kalman filter-based algorithm, to track a single target in range, has been designed and assessed. The proposed approach exploits spillover of target energy between consecutive matched filter samples.

In this work, we propose and assess an algorithm to track multiple targets in range and azimuth. It is the natural, though not trivial, extension of the Kalman filter-based algorithm, proposed in [5] to track a single target in range, to multitarget scenarios and to range-azimuth tracking. The main novelty of the proposed algorithm is the potential to deal with multiple targets in spatial proximity adopting a multitarget scheme as an alternative to the single target detector proposed in [3] that, in turn, has been modified to collect all useful target components in both range and azimuth.

This work was supported by CNIT within the "HABITAT" project (PON-011936) funded by MIUR.

The paper is organized as follows. Section II introduces the detection stage while Section III focuses on the tracking stage. Section IV deals with the performance assessment.

II. Design of a multitarget detector

A mechanically rotating reflector is assumed as radar antenna. It is mounted at a certain height above the sea level and illuminates the surveillance area transmitting a bandpass signal whose lowpass equivalent is a train of rectangular pulses of duration T_p. The rate at which observations are made in azimuth depends on the time for the antenna to make one rotation, namely $T_a = 2\pi/|\omega_a|$, where ω_a denotes the angular velocity of the antenna, in radians per seconds (rad/s), which we assume to be positive in case of counterclockwise rotation. Notice also that the number of consecutive pulses on a stationary target, N say, is (approximately) equal to $N = (\pi/180) \cdot (\Delta\theta_3)/(|\omega_a|T)$, where $\Delta\theta_3$ is the (-3 dB) beamwidth (in degrees) and T is the pulse repetition time (PRT). Typically, a discrete form for the signal corresponding to each range-azimuth cell is obtained by properly sampling the output of a filter matched to the transmitted pulse and fed by the received signal [6]. Thus, we can form an N-dimensional vector of samples representative of the received signal corresponding to the lth range gate, $l = 1, \dots, L$. To this end, it is customary to assume that the target is located exactly "where the matched filter is sampled"; however, the round-trip delay of the received signal is generally different from the sampling instants and, hence, there exists a residual delay that gives rise to a spillover of target energy. In other words, a target contributes to two consecutive range cells.

In the sequel we assume a multitarget scenario. Suppose that two targets are present at most. The generalization to an arbitrary, albeit known, number of targets is straightforward. Moreover, assume that the two closely spaced (point-like and slowly-fluctuating) targets are moving with constant radial velocity (and in the antenna far field) within three consecutive range cells, indexed by $l-1, l, l+1$. We denote by θ_i the azimuth of the ith target that is supposed to be approximately constant over the coherent processing interval. We also suppose that $\theta_m = (\theta_1 + \theta_2)/2$ is approximately known. Due to the presence of spillover there might be target energy also in the matched filter outputs corresponding to the $(l-2)$th and the $(l+2)$th range cells. Then, in order to collect most of the energy backscattered by the targets, it is reasonable to process samples at the output of the matched filter at the instants $t_{j,n} = t_{\min} + (j-1)T_p + nT$, $j = l-2, \dots, l+2$, $n = n_{\theta_m} - 3N/2, \dots, n_{\theta_m} + 5N/2 - 1$, where $t_{\min}$ represents the beginning of the sampling process while n_{θ_m} is given by

$$n_{\theta_m} = \text{round}\left(\frac{\theta_m + 2h\pi\ \text{sgn}(\omega_a) - \theta_{0a}}{\omega_a T}\right) - \frac{N}{2} \quad (1)$$

with θ_{0a} the angular position of the antenna at $t = 0$, h an integer indexing the antenna scan, $\text{sgn}(x)$ the signum of x, and $\text{round}(x)$ the integer closest to x. Thus time samples are grouped to form the $4N$-dimensional vector $\boldsymbol{z}_j = \boldsymbol{s}_j + \boldsymbol{n}_j$, $j = l-2, \ldots, l+2$, with $\boldsymbol{s}_j$ the signal component and $\boldsymbol{n}_j$ the noise component. It is not difficult to compute, following the lead of [3], [4], the contribution, $\boldsymbol{s}_{i,j} \in \mathbb{C}^{4N\times 1}$ say, of the ith target to the jth range cell, $j = l-2, \ldots, l+2$, up to a complex factor α_i taking into account target and channel effects. Obviously, $\boldsymbol{s}_{i,j}$ depends on the range cell the target belongs to, the "residual delay" from the center of its range cell, ϵ_i say, its normalized Doppler shift, ν_i say, and θ_i. In particular, it is proportional to the steering vector:

$$\boldsymbol{v}(\nu_i, \theta_i) = \frac{1}{\sqrt{N}}[\underbrace{0\cdots 0}_{3N/2+r}\ c_{\theta_i}(n_{\theta_i})\ c_{\theta_i}(n_{\theta_i}+1)e^{\sqrt{-1}\ 2\pi\nu_i} \cdots\ c_{\theta_i}(n_{\theta_i}+N-1)e^{\sqrt{-1}\ 2\pi(N-1)\nu_i}\ \underbrace{0\cdots 0}_{3N/2-r}]' \quad (2)$$

where $c_{\theta_i}(n_{\theta_i})$ takes into account the amplitude modulation due to antenna rotation, $r \in \{-3N/2, \ldots, 3N/2\}$ represents an index taking into account quantization of targets' azimuths, and $'$ denotes transpose. It follows that the signal component $\boldsymbol{s}_j$, $j = l-2, \ldots, l+2$, is given by

$$\boldsymbol{s}_j(j_1, j_2, \epsilon_1, \epsilon_2, \nu_1, \nu_2, \theta_1, \theta_2) = \sum_{i=1}^{2} \alpha_i \boldsymbol{s}_{i,j}(j_i, \epsilon_i, \nu_i, \theta_i)$$

where $j_i \in \{l-1, l, l+1\}$ denotes the range cell the ith target belongs to. We also assume that signal returns are buried in zero mean, complex normal noise, independent from range cell to range cell, with covariance matrix $\sigma^2 \boldsymbol{I}_{4N}$, where $\boldsymbol{I}_m$ is the m-dimensional identity matrix. In symbols, $\boldsymbol{n}_j \sim \mathcal{CN}(\boldsymbol{0}, \sigma^2 \boldsymbol{I}_{4N})$ with σ^2 an unknown parameter.

Summarizing, the problem at hand is that of detecting the possible presence of two targets and of estimating the parameters of interest, namely j_1, j_2, ϵ_1, ϵ_2, ν_1, ν_2, θ_1, and θ_2, together with the nuisance parameters α_1, α_2, and σ^2. In order to formulate and eventually solve the estimation problem we can now define an augmented received vector

$$\tilde{\boldsymbol{z}} = [\boldsymbol{z}'_{l-2}\ \boldsymbol{z}'_{l-1}\ \boldsymbol{z}'_{l}\ \boldsymbol{z}'_{l+1}\ \boldsymbol{z}'_{l+2}]' \in \mathbb{C}^{20N\times 1}.$$

Accordingly, we can define an augmented steering vector, corresponding to the ith target, $\boldsymbol{h}_i(j_i, \epsilon_i, \nu_i, \theta_i) \in \mathbb{C}^{20N\times 1}$ say. In addition, the hypothesis test to be solved is

$$\begin{cases} H_0 : \tilde{\boldsymbol{z}} = \tilde{\boldsymbol{n}} \\ H_1 : \tilde{\boldsymbol{z}} = \sum_{i=1}^{2} \alpha_i \boldsymbol{h}_i(j_i, \epsilon_i, \nu_i, \theta_i) + \tilde{\boldsymbol{n}} = \boldsymbol{H}(\boldsymbol{x}_1, \boldsymbol{x}_2)\boldsymbol{x}_3 + \tilde{\boldsymbol{n}} \end{cases}$$

where $\boldsymbol{H}(\boldsymbol{x}_1, \boldsymbol{x}_2) = [\boldsymbol{h}_1(j_1, \epsilon_1, \nu_1, \theta_1)\ \ \boldsymbol{h}_2(j_2, \epsilon_2, \nu_2, \theta_2)]$ is assumed to be a full-column-rank matrix, with $\boldsymbol{x}_1 = [j_1\ j_2\ \epsilon_1\ \epsilon_2\ \theta_1\ \theta_2]'$, $\boldsymbol{x}_2 = [\nu_1\ \nu_2]'$, and $\boldsymbol{x}_3 = [\alpha_1\ \alpha_2]'$. Obviously, $\tilde{\boldsymbol{n}} \sim \mathcal{CN}(\boldsymbol{0}, \sigma^2 \boldsymbol{I}_{20N})$ (with σ^2 an unknown parameter). Thus, leaving aside for the moment the unknown parameters ν_1, ν_2, the above hypothesis test can be solved through the generalized likelihood ratio test (GLRT) that assumes the intermediate form

$$\max_{\boldsymbol{x}_1} \frac{\tilde{\boldsymbol{z}}^\dagger \boldsymbol{P}_{\boldsymbol{H}}(\boldsymbol{x}_1, \boldsymbol{x}_2)\tilde{\boldsymbol{z}}}{\tilde{\boldsymbol{z}}^\dagger \tilde{\boldsymbol{z}}} \underset{H_0}{\overset{H_1}{\gtrless}} \gamma \quad (3)$$

where $\boldsymbol{P}_{\boldsymbol{H}}(\boldsymbol{x}_1, \boldsymbol{x}_2)$ is the projection matrix onto the space spanned by the columns of the matrix $\boldsymbol{H}(\boldsymbol{x}_1, \boldsymbol{x}_2)$ and γ denotes a threshold to be set in order to ensure the desired probability of false alarm (P_{fa}).

It still remains to overcome the uncertainty on ν_1 and ν_2. To this end, we use a suboptimum procedure. In fact, neglecting the actual expression of the spillover term to adjacent range cells, we can model the received signal in the jth range cell, $j = l-2, \ldots, l+2$, as

$$\boldsymbol{z}_j = [\boldsymbol{v}(\nu_1, \theta_1)\ \boldsymbol{v}(\nu_2, \theta_2)]\,\boldsymbol{u}_j + \boldsymbol{n}_j \in \mathbb{C}^{4N\times 1}$$

with $\boldsymbol{v}$ given by (2), $\boldsymbol{u}_j = [\alpha_{1,j}\ \alpha_{2,j}]'$, and $\boldsymbol{n}_j \sim \mathcal{CN}\left(\boldsymbol{0}, \sigma^2 \boldsymbol{I}_{4N}\right)$. It turns out that the ML estimate of $\boldsymbol{x}_2$, $\widehat{\boldsymbol{x}}_2 = [\widehat{\nu}_1, \widehat{\nu}_2]'$ say, is given by

$$\widehat{\boldsymbol{x}}_2 = \arg\max_{\nu_1, \nu_2} \max_{\theta_1, \theta_2} \sum_{j=l-2}^{l+2} \boldsymbol{z}_j^\dagger \boldsymbol{P}(\nu_1, \nu_2, \theta_1, \theta_2)\boldsymbol{z}_j \quad (4)$$

where $\boldsymbol{P}(\nu_1, \nu_2, \theta_1, \theta_2)$ is the projection matrix onto the space spanned by the columns of the matrix $[\boldsymbol{v}(\nu_1, \theta_1)\ \boldsymbol{v}(\nu_2, \theta_2)]$, $(\nu_1, \theta_1) \neq (\nu_2, \theta_2)$, $\nu_i \in \{0, 1/M, \ldots, (M-1)/M\}$. Then, we plug the estimated pair of normalized Doppler frequencies $\widehat{\boldsymbol{x}}_2$ into the above detector (3), in place of $\boldsymbol{x}_2$.

A few final remarks are in order. First, observe that maximization over $\boldsymbol{x}_1 = [j_1\ j_2\ \epsilon_1\ \epsilon_2\ \theta_1\ \theta_2]'$ cannot be conducted in closed form. We thus resort to a grid search to maximize with respect to such parameters. Second, the GLRT and its ad hoc implementation guarantee the constant false alarm rate (CFAR) property with respect to σ^2.

III. Tracking stage

Assume that radar data are available over $[0, +\infty)$. Moreover, assume that the motion of each target can be modeled according to a nearly constant velocity model along x and y. More precisely, we suppose that the kinematics of the ith target is ruled by the following state space model

$$\begin{cases} \boldsymbol{x}_i(k+1) &= \boldsymbol{F}\boldsymbol{x}_i(k) + \boldsymbol{w}_{1i}(k) \\ \boldsymbol{y}_i(k) &= \boldsymbol{K}\boldsymbol{x}_i(k) + \boldsymbol{w}_{2i}(k) \end{cases}$$

with k denoting the kth antenna scan and $\boldsymbol{x}_i(k) = [x_i(k)\ v_{xi}(k)\ y_i(k)\ v_{yi}(k)]'$; $x_i(k)$ and $y_i(k)$ are the cartesian coordinates of the target over $(T_{k,i}, T_{k,i} + NT)$, namely the time interval during which the target is within the (-3 dB) antenna beamwidth, while $v_{xi}(k)$ and $v_{yi}(k)$ are the target velocity components along x and y over the same time interval; $\boldsymbol{y}_i(k) = [x_i(k)\ y_i(k)]'$,

$$\boldsymbol{F} = \text{diag}\left(\boldsymbol{F}_1, \boldsymbol{F}_1\right), \ \boldsymbol{F}_1 = \begin{bmatrix} 1 & T_a \\ 0 & 1 \end{bmatrix}, \ \boldsymbol{K} = \begin{bmatrix} 1 & 0 & 0 & 0 \\ 0 & 0 & 1 & 0 \end{bmatrix}$$

As to $\boldsymbol{w}_{1i}(k)$ and $\boldsymbol{w}_{2j}(k)$, they are assumed to be (approximately) independent, zero-mean normal sequences. Moreover, we have that

$$E[\boldsymbol{w}_{1i}(k)\boldsymbol{w}'_{1j}(h)] = \boldsymbol{Q}\delta_{ij}\delta_{kh}, \ E[\boldsymbol{w}_{2i}(k)\boldsymbol{w}'_{2j}(h)] = \boldsymbol{R}\delta_{ij}\delta_{kh}$$

with $\boldsymbol{Q} = \mathrm{diag}(\boldsymbol{Q}_1, \boldsymbol{Q}_1)$ where $\boldsymbol{Q}_1$ is given in [7] and δ_{ij} the Kronecker symbol. $\boldsymbol{Q}_1$ can be set based on the maximum tolerable difference between the nominal and the actual target velocity component (along x or y), $\Delta v_{\max}$ say, over the "sampling interval" T_a. Similarly, $\boldsymbol{R} = \mathrm{diag}(\boldsymbol{R}_1, \boldsymbol{R}_1)$. As to $\boldsymbol{R}_1$, it can be chosen based on an educated guess on the second-order moments of the measurement errors.

In order to describe the main ideas underlying the proposed multitarget tracker, denote by $\mathcal{N}_k$, $k \geq 2$, the set of (positive) integers indexing the tracks that are active over the kth antenna scan (i.e., confirmed and to-be-confirmed ones).

1) Over the kth scan, for the ith track, $i \in \mathcal{N}_k$, we compute the one step prediction of the state, $\widehat{\boldsymbol{x}}_i(k+1|k)$ say, and the associated error covariance matrix by implementing the Kalman filter (KF) equations.

2) Based on the predicted positions of targets over the $(k+1)$th scan (corresponding to active tracks over the kth scan) we construct a partition of $\mathcal{N}_k$, $\mathcal{N}_k^1, \ldots, \mathcal{N}_k^{m_k}$ say, in order to determine targets that might be in close spatial proximity and, hence, groups of range-azimuth cells to be jointly processed by the detection stage; the partition is constructed according to a given criterion (subsequently described).

3) If the cardinality of $\mathcal{N}_k^j$, $j = 1, \ldots, m_k$, is greater than one, the multitarget decision scheme is used to detect and localize the targets whose indices are in $\mathcal{N}_k^j$; otherwise, we use a single target detector based on [3] and properly adapted to the case at hand. At this point we have a set of measurements for the $(k+1)$th scan, $\mathcal{M}_{k+1}$ say.

4) $\mathcal{M}_{k+1}$ is fed to a non parametric joint probabilistic data association (JPDA) algorithm [7].

5) The state of each track is updated: a to-be-confirmed track can be confirmed (otherwise, it is deleted) using an m_c/n_c rule, i.e., we confirm a track the first time the number of detections over the last n_c scans is greater than or equal to m_c; similarly, a confirmed track can be deleted using an m_d/n_d rule. In addition, tracks in $\mathcal{N}_k^j$, $j = 1, \ldots, m_k$, are compared to merge possible "close tracks": $\forall r, s \in \mathcal{N}_k^j$, $r < s$, $j = 1, \ldots, m_k$, if the rth track is close in position and velocity to the sth track, the former is deleted. In formulas, if $[(x_r(k) - x_s(k))^2 + (y_r(k) - y_s(k))^2]^{1/2}$ is less than a threshold value Th_{pos} and $[(v_{xr}(k) - v_{xs}(k))^2 + (v_{yr}(k) - v_{ys}(k))^2]^{1/2}$ is less than a threshold value Th_{vel} the rth track is deleted.

6) After existing tracks have been updated, we run a conventional detector over remaining range-azimuth cells of the surveillance region. Range-azimuth cells "occupied by targets" associated with active tracks, but also cells surrounding the above estimated target positions, are not scanned by the conventional detector; notice that it is necessary to set guard cells (not fed to the more conventional detector) to avoid that the spillover due to (already detected) strong targets might originate additional false targets. Thus, if $\widehat{l}$ and $\widehat{\theta}$ are the estimated range cell and azimuthal position of the target corresponding to an active track, respectively, the conventional detector does not scan range cells $\widehat{l}$, $\widehat{l} - 1$, and $\widehat{l} + 1$ together with (at least) pulses $n_{\widehat{\theta}} - N/2, \ldots, n_{\widehat{\theta}} + 3N/2 - 1$. The conventional detector is the cascade of two detectors: the observables corresponding to each range-azimuth cell within the area of interest are fed to a first stage designed assuming the presence of a target "matched to" the lth range cell and the hth azimuth cell. If a target is detected, setting the threshold to guarantee $P_{fa} = 10^{-2}$, the observables are fed to the single target detector of item 3. Again, the threshold is set to guarantee $P_{fa} = 10^{-2}$.

7) The tracker initiates potential tracks over the $(k+1)$th scan in case of detections (which come from the detector described in the previous item) over the kth and the $(k+1)$th scans corresponding to range-azimuth cells in spatial proximity. More precisely, assume that a new target has been detected over the kth and the $(k+1)$th scan and denote by $(\tilde{x}(k)\ \tilde{y}(k))$ and $(\tilde{x}(k+1)\ \tilde{y}(k+1))$ its estimated position over the kth and the $(k+1)$th scan, respectively; moreover, assume that the Euclidean distance between the above points is less than $v_{\max} T_a$, with $v_{\max}$ denoting the maximum admissible target velocity; then, such measurements can be interpreted as originated by the same target and give rise to a new (to be confirmed) track. More generally, in presence of multiple detections over the kth scan and/or the $(k+1)$th scan, we initiate new tracks for a subset of available candidates. To this end, we compute all distances between detections over consecutive scans and, among those compatible with the maximum admissible target velocity, choose the pair with the smallest distance; then, after discarding all pairs having the first or the second point in common with the selected one, we choose the pair with the smallest distance among the survivors, and so on. The same rationale is used to initiate tracks over the second scan based on possible detections over the first two scans (which come from the detector described in the previous item).

At this point $\mathcal{N}_{k+1}$ contains the set of (positive) integers indexing the active tracks over $(k+1)$th scan.

It still remains to specify how to partition $\mathcal{N}_k$. To this end, denote by $d(\boldsymbol{x}, \boldsymbol{y})$ the Euclidean distance between $\boldsymbol{x}$ and $\boldsymbol{y}$ and by $d_0 > 0$ a given threshold. In particular, we investigate the following partition rule that, leading to sets consisting of one or two elements, keeps the computational complexity of the detection stage at a low level (we assume that the cardinality of $\mathcal{N}_k$ is greater than one):

1) set $\mathcal{N}' = \mathcal{N}_k$ and $j = 1$.

2) Construct the set of distances, $\mathcal{D}$ say, between any two elements $\widehat{\boldsymbol{y}}_r(k+1|k)$ and $\widehat{\boldsymbol{y}}_s(k+1|k)$ of the set $\{\widehat{\boldsymbol{y}}_i(k+1|k), i \in \mathcal{N}'\}$ that satisfy the following additional constraints $|l_r - l_s| \leq 2$ and $|n_{\theta_r} - n_{\theta_s}| \leq 3N$, where l_i and θ_i denote the range cell and the azimuthal position of the target corresponding to the ith track in $\mathcal{N}'$.

3) Compute the minimum among such distances, i.e., $d_j = \min \mathcal{D}$ (remember that the minimum is equal to $+\infty$ for an empty set): if such a minimum is different from $+\infty$, let $\mathcal{N}_k^j = \{r_1, r_2\}$ where r_1 and r_2 are such that $d(\widehat{\boldsymbol{y}}_{r_1}(k+1|k), \widehat{\boldsymbol{y}}_{r_2}(k+1|k)) = d_j$; otherwise construct a singleton for any element of $\{\widehat{\boldsymbol{y}}_r(k+1|k), r \in \mathcal{N}'\}$ and quit the loop.

4) Compute the new $\mathcal{N}'$ as $\mathcal{N}' = \mathcal{N}' \setminus \{r_1, r_2\}$ if $\mathcal{N}'$ is an empty set quit the loop; if, instead, the cardinality of $\mathcal{N}'$ is one, let $\mathcal{N}_k^{j+1} = \{r, r \in \mathcal{N}'\}$ and quit the loop; otherwise, let $j = j + 1$ and return to step 2.

IV. Performance Assessment and conclusions

In this section, we assess the performance of the tracker by simulation techniques. All the illustrative examples assume the following values for the relevant parameters: $f_c = 9.375$ GHz, $T_p = 0.2$ μs, $1/T = 3$ kHz, $\omega_a = \pi$ rad/s, $\Delta\theta_3 = 0.36°$, $N = 6$, $q = 1$ m^2/s^3, $\boldsymbol{R}_1 = 5$ m^2, $m_c = 5$, $n_c = 8$, $m_d = 1$, $n_d = 8$, $v_{\max}T_a = 60$ m, $Th_{pos} = 3$ m, and $Th_{vel} = 1$ m/s. The trajectories of the targets are depicted in Fig. 1 where we assume a constant acceleration model; markers indicate the position of each target at scans multiple of 5. Notice the crossing of three targets around scan 50 and concerning the two targets moving along parallel trajectories the overtake of the left one on the right one in between scans 45 and 55. Moreover, we define the signal-to-noise ratio (SNR) for the ith target as $\text{SNR}_i = |\alpha_i|^2/\sigma^2$ with $\sigma^2 = 1$. Figs. 2-3 refer to the case of targets with the same strength while in Figs. 4-5 one of the three targets whose trajectories cross each other is weaker than the others (the one moving from top-right to bottom-left); similarly, one of the two targets moving along parallel trajectories is weaker than the other (the one on the right). For comparison purposes the performance of a tracker that employs the single target detector even for targets in spatial proximity is considered too. In Figs. 2-5 actual trajectories are in blue, estimated ones in green for the proposed tracker and in red for the competitor. The proposed tracker seems to outperform the competitor; in fact, in the considered examples it is more effective to track close targets.

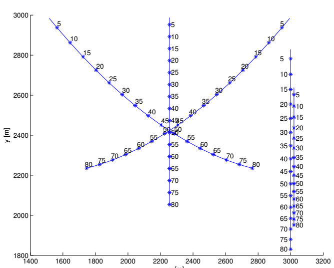

Fig. 1. Simulated trajectories.

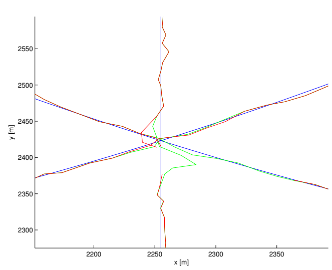

Fig. 2. Tracking results assuming targets with equal strength. SNR=20 dB.

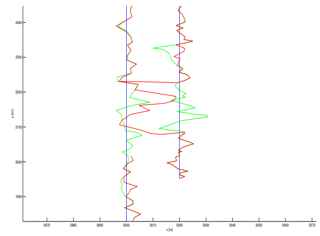

Fig. 3. Tracking results assuming targets with equal strength. SNR=20 dB.

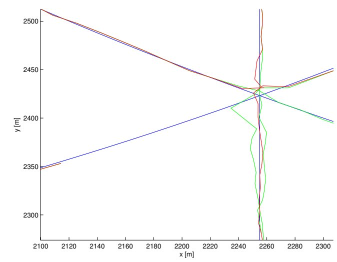

Fig. 4. Tracking results assuming two strong targets (SNR=30 dB) and a weaker one (SNR=20 dB).

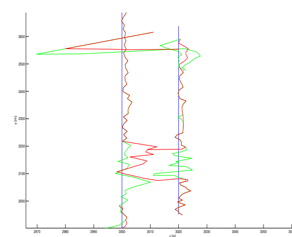

Fig. 5. Tracking results assuming a strong target (SNR=30 dB) and a weaker one (SNR=20 dB).

References

[1] X. Zhang, P. K. Willett, Y. Bar-Shalom, "Monopulse Radar Detection and Localization of Multiple Unresolved Targets via Joint Bin Processing," *IEEE Trans. Sig. Proc.*, Vol. 53, No. 4, pp. 1225-1236, Apr. 2005.

[2] X. Zhang, P. K. Willett, Y. Bar-Shalom, "Detection and Localization of Multiple Unresolved Extended Targets via Monopulse Radar Signal Processing," *IEEE Trans. AES*, Vol. 45, No. 2, pp. 455-472, Apr. 2009.

[3] D. Orlando, G. Ricci, "Adaptive radar detection and localization of a point-like target," *IEEE Trans. Sig. Proc.*, Vol. 59, No. 9, pp. 4086-4096, Sept. 2011.

[4] F. Bandiera, M. Mancino, G. Ricci, "Localization strategies for multiple point-like radar targets," *IEEE Trans. Sig. Proc.*, Vol. 60, No. 12, pp. 6708-6712, Dec. 2012.

[5] M. Del Coco, D. Orlando, G. Ricci, "A tracking system exploiting interaction between a detector with localization capabilities and the KF," *IEEE Trans. Sig. Proc.*, Vol. 60, No. 11, pp. 6031-6036, Nov. 2012.

[6] F. Bandiera, D. Orlando, G. Ricci, *Advanced radar detection schemes under mismatched signal models*, Series on Synthesis Lectures on Signal Processing, Vol. 8, Morgan & Claypool Publishers, 2009.

[7] Y. Bar-Shalom, T. E. Fortmann, *Tracking and Data Association*, Academic Press, 1988.